ZEUS High-Q^2 and BSM group.
Summary of the group results to be presented at the EPS 2007 Conference

Inclusive NC and CC cross sections at high-Q^2 and EW physics

1 High-Q^2 neutral and charged current $e^{\pm}p$ DIS cross sections with longitudinally polarised lepton beams

1.1 NC cross sections with polarized e^-p data

The neutral current cross sections for deep inelastic scattering in e^-p collisions at HERA with longitudinally polarised electron beams have been measured. The results are based on an integrated luminosity of $177\,\mathrm{pb}^{-1}$ collected by the ZEUS detector in 2005 and 2006 at a centre-of-mass energy of 318 GeV. Single differential cross sections with respect to Q^2, x and y have been measured for $Q^2 > 185\,\mathrm{GeV}^2$ with the entire data sample and separately for positive and negative values of the longitudinal polarisation of the electron beam. Parity violation is highlighted in the charged dependent polarisation asymmetry. The reduced cross section has been measured in the kinematic region $200\,\mathrm{GeV}^2 < Q^2 < 30\,000\,\mathrm{GeV}^2$ and $0.005 < x < 0.65$ separately for positive and negative polarisations and at zero polarisation by correcting the residual polarisation of the combined data set. These measurements have been combined with the previously measured ZEUS e^+p NC cross sections to extract the structure function xF_3.

Figures: Fig. 1 to Fig. 8
Comments: Preliminary results presented at the DIS 2007 Workshop. For additional informations see S. Bhadra presentation [1] at DIS 2007.

1.2 CC cross sections with polarized e^-p data

The cross sections for charged current deep inelastic scattering in e^-p collisions with a longitudinally polarised electron beam have been measured. The measurements are based on a data sample collected with the ZEUS detector at HERA in 2004 and 2005 at a centre-of-mass energy of 318 GeV. The total cross section is presented at positive and negative values of the longitudinal polarisation of the electron beam, with an estimate of the right-handed CC DIS cross section and a limit on the mass of a right-handed W boson. In addition, the differential cross sections and the reduced cross sections are presented in the kinematic region $Q^2 > 200\,\mathrm{GeV}^2$.The measured cross sections are well described by the predictions of the Standard Model.

Figures: Fig. 9 to Fig. 12
Comments: Preliminary results presented at the ICHEP06. For additional information see the ZEUS contributed paper [2] to ICHEP06. An update of this analysis, including the full 2004-2006 e^-p sample ($175\,\mathrm{pb}^{-1}$), may become available in time for EPS 2007.

1.3 NC and CC cross sections with polarized e^+p data

The cross sections for charged and neutral current deep inelastic scattering in e^+p collisions with longitudinally polarised positron beams have been measured using the ZEUS detector at HERA. The results, based on data collected in the 2006-2007 data taking period, correspond to an integrated luminosity of $120\,\mathrm{pb}^{-1}$ at a centre-of-mass energy of 318 GeV. The single differential cross sections, which are presented for the kinematic region $Q^2 > 200\,\mathrm{GeV}^2$ and for both positive and negative values of the longitudinal polarisation of the positrom beam, are compared to the predictions of the Standard Model.

Figures: None
Comments: Results not yet released. May become available in time for EPS 2007.

1.4 H1 and ZEUS combined NC High-Q^2 cross sections

Measurements by the H1 and ZEUS Collaborations of the NC cross sections of deep inelastic polarised electron and positron-proton scattering are combined in order to investigate the interference of weak and electromagnetic interactions at high four-momentum transfer squared, Q^2. The data provide the most accurate measurements of the interference structure function $xF_3^{\gamma Z}$, which is sensitive to the valence quark distributions down to lower values of Bjorken x. The data on polarised cross sections asymmetries, $A^{\pm}$, lead to the first observation of parity violation in neutral current $e^{\pm}p$ scattering at distances down to 10^{-18} m.

Figures: Figs. 13 and 14
Comments: H1 and ZEUS combined contributed paper [3] to ICHEP06.
An update of these results, including newly measured H1 and ZEUS high-Q^2 NC e^-p cross sections, may become available in time for EPS 2007.

1.5 QCD and Electroweak analysis of the ZEUS NC and CC inclusive and jet cross sections

The precision and kinematic coverage of the ZEUS inclusive and jet cross section measurements make now possible to perform QCD and EW fits with the simultaneous determination of the proton PDFs and the electroweak parameters. In this analysis the neutral current vector and axial vector couplings have been determined in a series of simultaneous fits with the PDF parameters. The axial couplings are dominantly constrained by unpolarised data, whereas the polarised e^-p data provide significant constraints on the vector couplings. These determination of the EW couplings are competitive in precision with those of the LEP experiments in the light-quark sector, and because they derive from $\gamma - Z^\circ$ interference they do not suffer from the sign ambiguity of the LEP results.

Figures: Figs. 15 and 16
Comments: Preliminary results presented at the ICHEP06. For additional information see the ZEUS contributed paper [4] to ICHEP06. With respect to the ICHEP06 version, Figures 15 and 16 now include new contours presented by the H1 Collaboration at DIS 2007.

References

[1] S. Bhadra, *NC cross sections with polarized $e^{-}p$ data.* Presented on behalf of the ZEUS Collaboration to the DIS 2007 Workshop, available on http://indico.cern.ch/contributionDisplay.py?contribId=35&sessionId=14&confId=9499.

[2] ZEUS-prel-06-022, contributed paper to ICHEP 2006, available on http://www-zeus.desy.de/physics/exo/ZEUS_PUBLIC/ichep06/pol-cc/ZEUS-prel-06-002.ps.

[3] H1prelim-06-142 and ZEUS-prel-06-022, H1 and ZEUS combined contributed paper to ICHEP 2006, available on http://www-zeus.desy.de/physics/exo/ZEUS_PUBLIC/ichep06/ewnc-h1zeus/ZEUS-prel-06-022.ps.

[4] ZEUS-prel-06-003, contributed paper to ICHEP 2006, available on http://www-zeus.desy.de/physics/phch/conf/ichep06/hiq2/10/ZEUS-prel-06-003.ps.

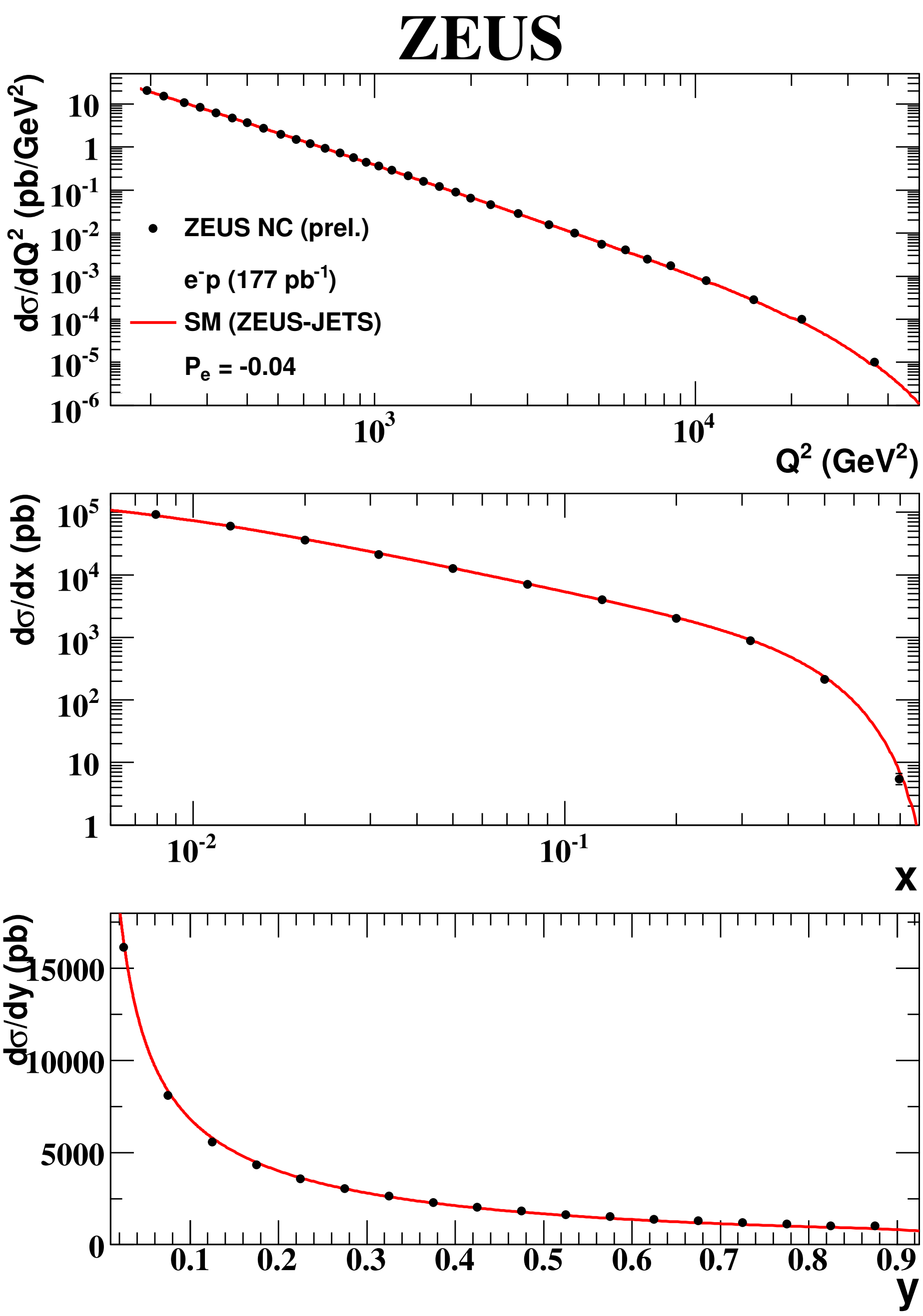

Figure 1: *The e^-p NC DIS cross section $d\sigma/dQ^2$, $d\sigma/dx$ and $d\sigma/dy$ for the entire e^-p data set. The closed circles represent data points and the curves show the predictions of the SM evaluated using the ZEUS-JETS PDFs at a polarisation corresponding to the residual polarisation of the data.*

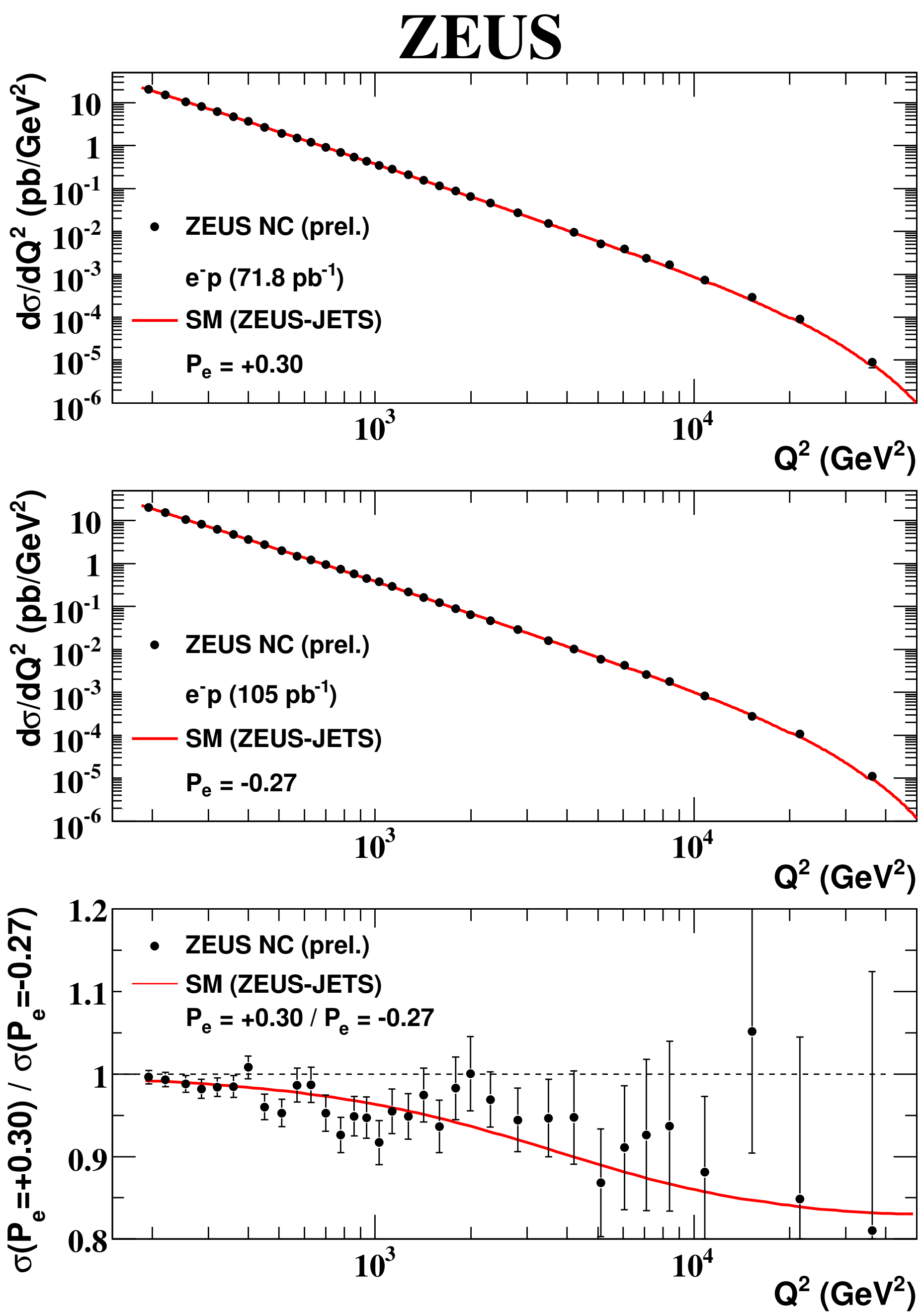

Figure 2: *The $e^{-}p$ NC DIS cross section $d\sigma/dQ^2$ for (top) positive polarisation data and (middle) negative polarisation data and (bottom) the ratio of the two. The closed circles represent data points and the curves show the predictions of the SM evaluated using the ZEUS-JETS PDFs. Only statistical uncertainties are shown in the cross section ratio measurement.*

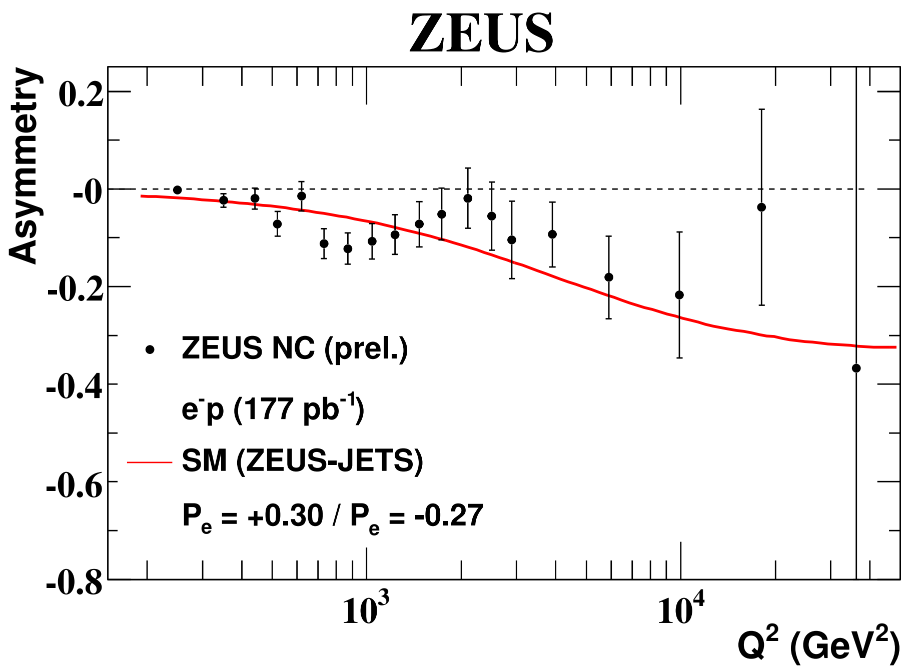

Figure 3: *Measurements of the polarisation asymmetry A^- as a function of Q^2. The closed circles represent data points and the curves show the predictions of the SM evaluated using the ZEUS-JETS PDFs. Only statistical uncertainties are shown.*

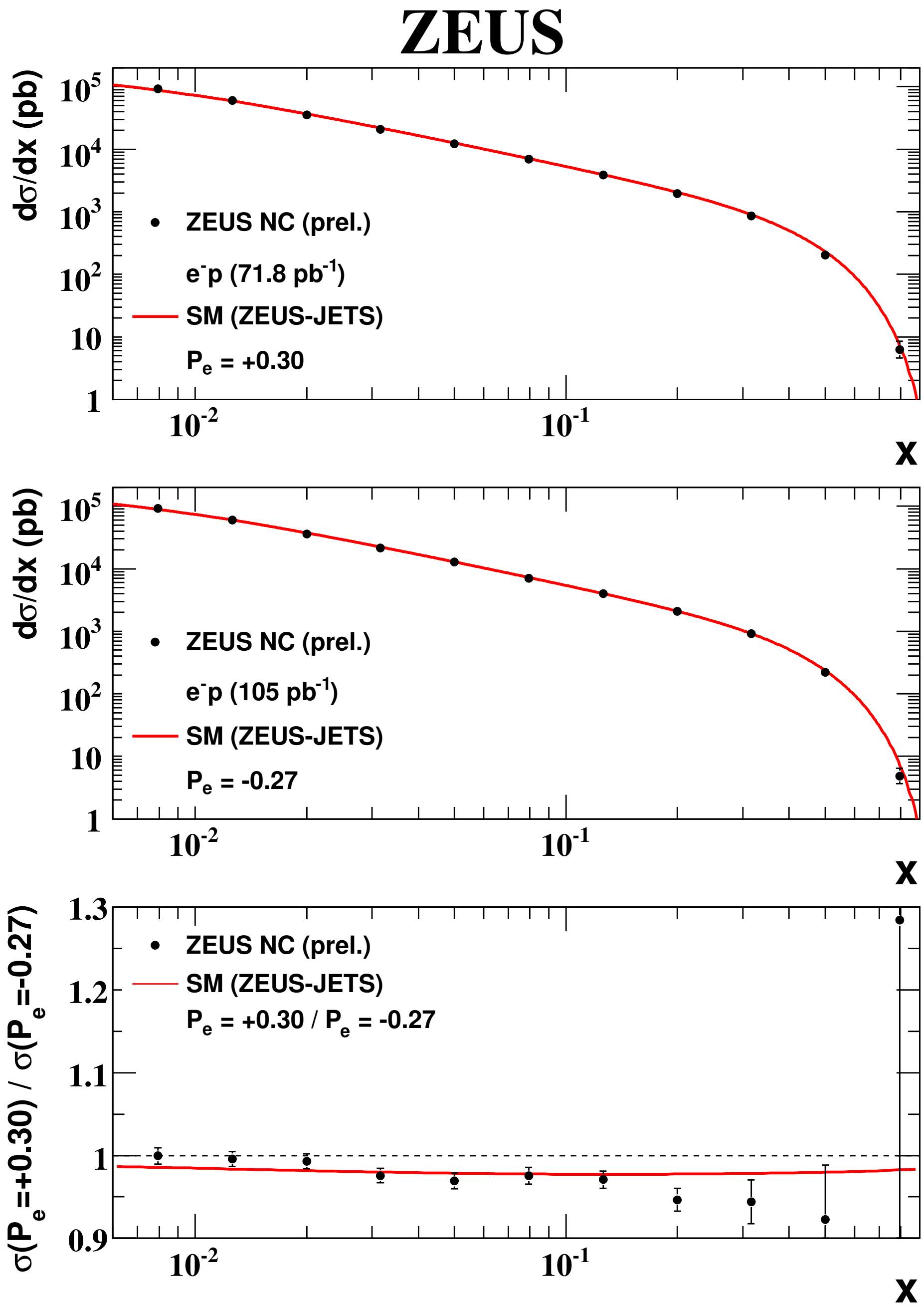

Figure 4: *The e^-p NC DIS cross section $d\sigma/dx$ for (top) positive polarisation data and (middle) negative polarisation data and (bottom) the ratio of the two. The closed circles represent data points and the curves show the predictions of the SM evaluated using the ZEUS-JETS PDFs. Only statistical uncertainties are shown in the cross section ratio measurement.*

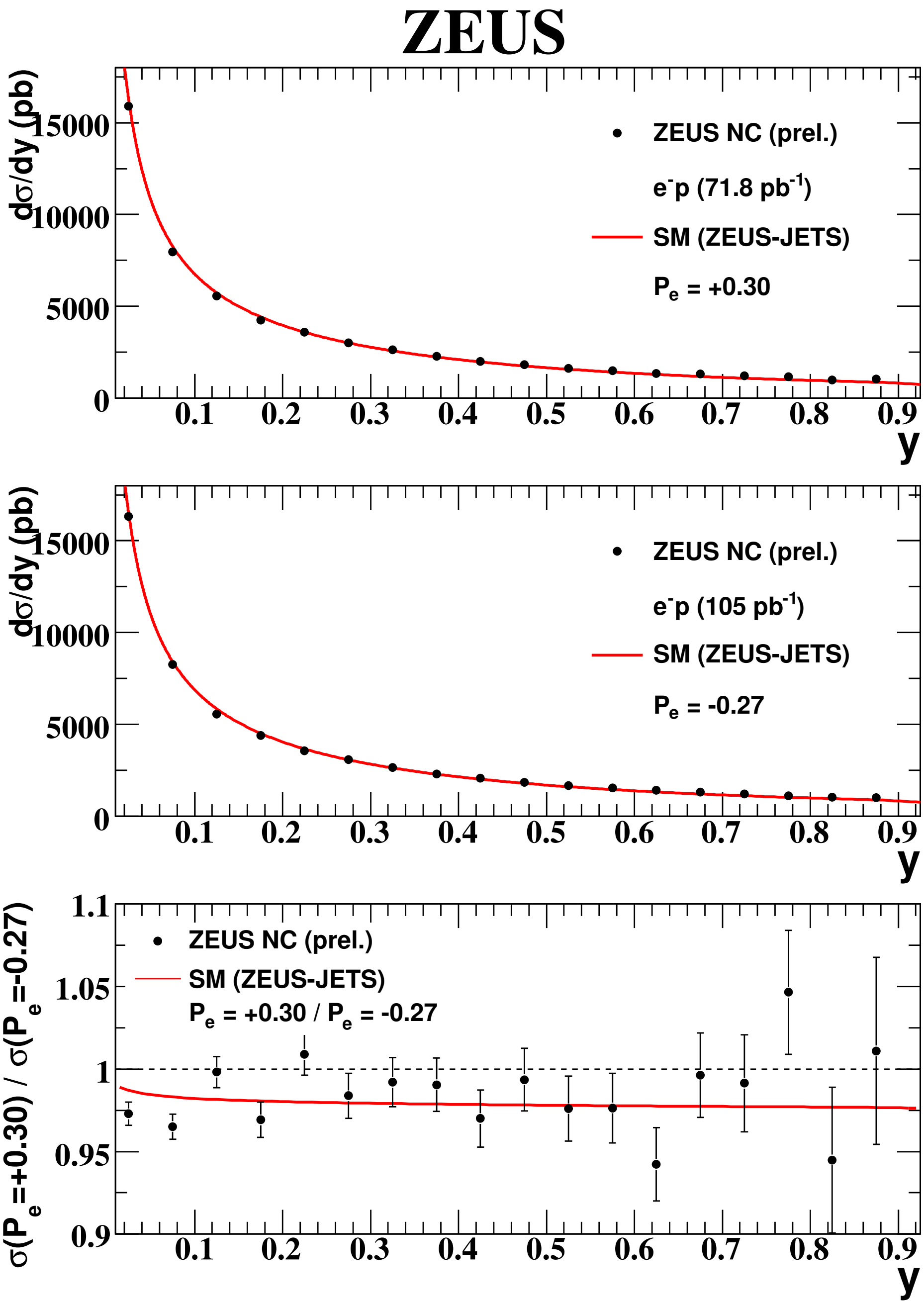

Figure 5: *The e^-p NC DIS cross section $d\sigma/dy$ for (top) positive polarisation data and (middle) negative polarisation data and (bottom) the ratio of the two. The closed circles represent data points and the curves show the predictions of the SM evaluated using the ZEUS-JETS PDFs. Only statistical uncertainties are shown in the cross section ratio measurement.*

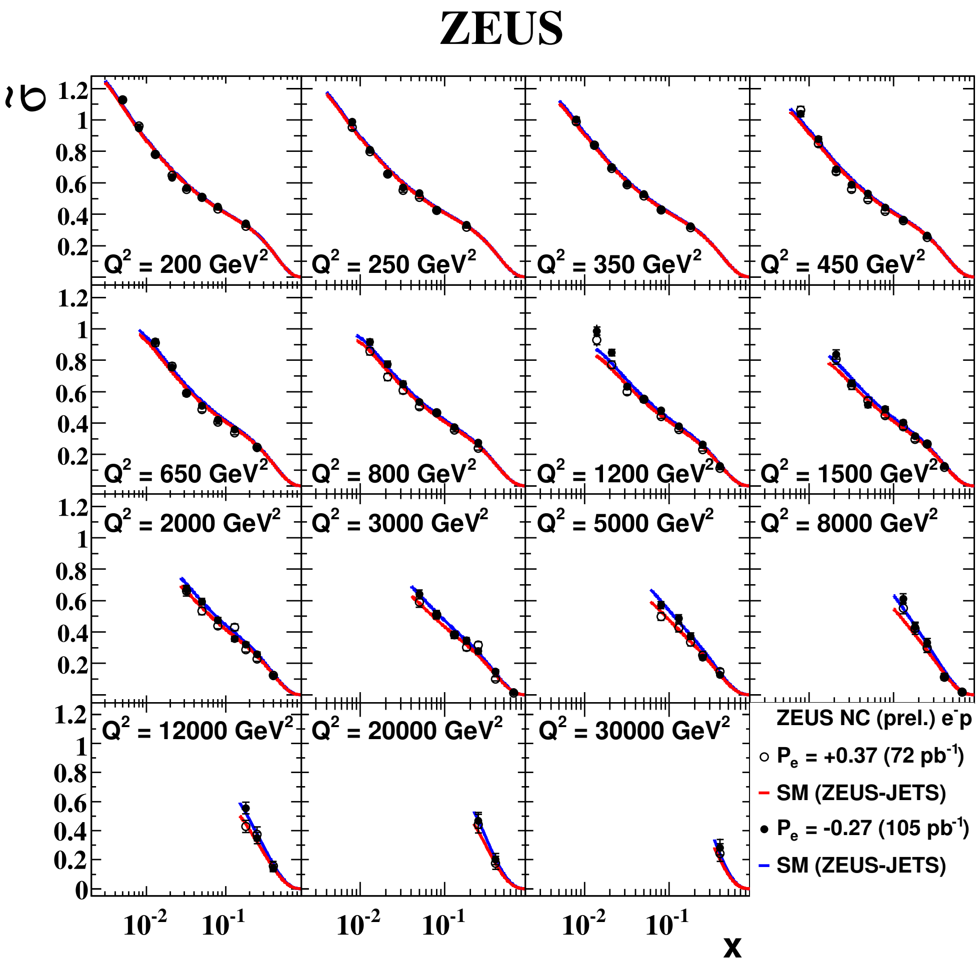

Figure 6: *The e^-p NC DIS reduced cross section $\tilde{\sigma}$ for positively and negatively polarised data plotted as a function of x in fixed Q^2 bins. The closed (open) circles represent data points for the negative (positive) polarisation measurements and the curves show the predictions of the SM evaluated using the ZEUS-JETS PDFs.*

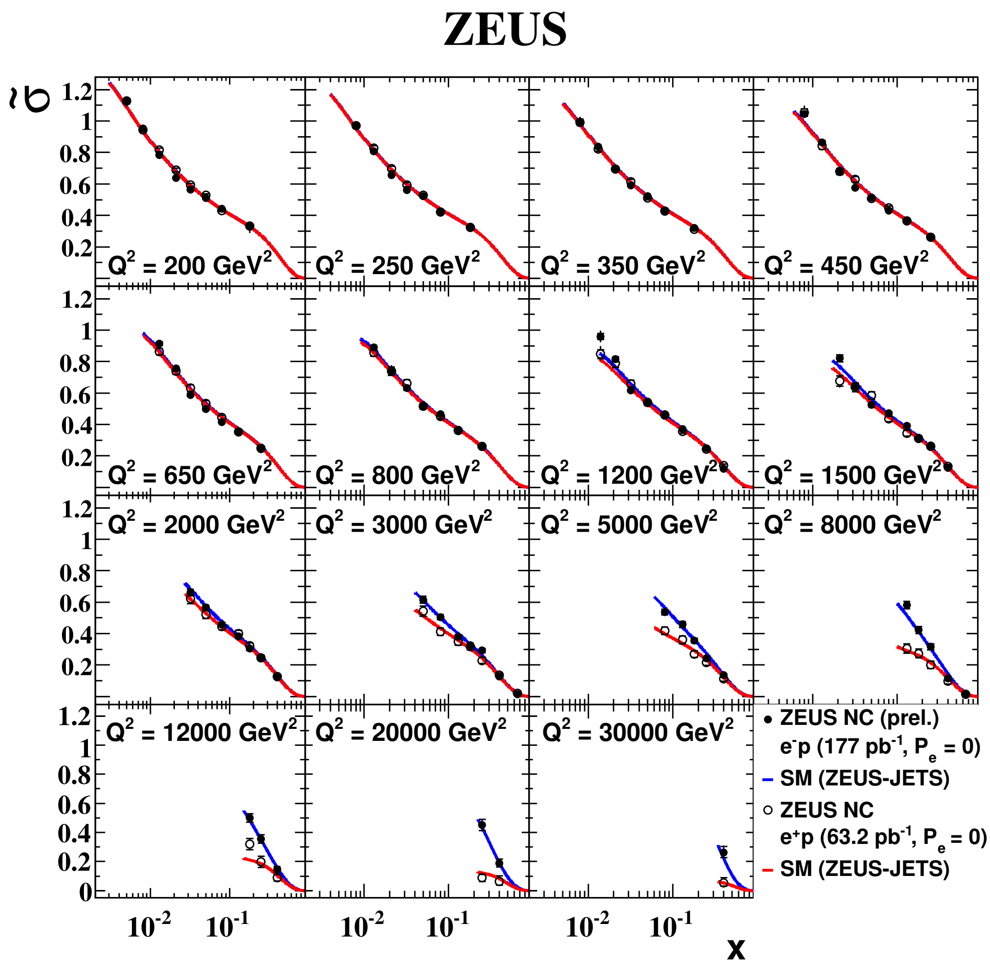

Figure 7: *The $e^{\pm}p$ unpolarised NC DIS reduced cross section $\tilde{\sigma}$ plotted as a function of x in fixed Q^2 bins. The closed (open) circles represent data points for e^-p (e^+p) collisions and the curves show the predictions of the SM evaluated using the ZEUS-JETS PDFs. The unpolarised e^-p reduced cross section is measured by correcting the residual polarisation using theoretical predictions.*

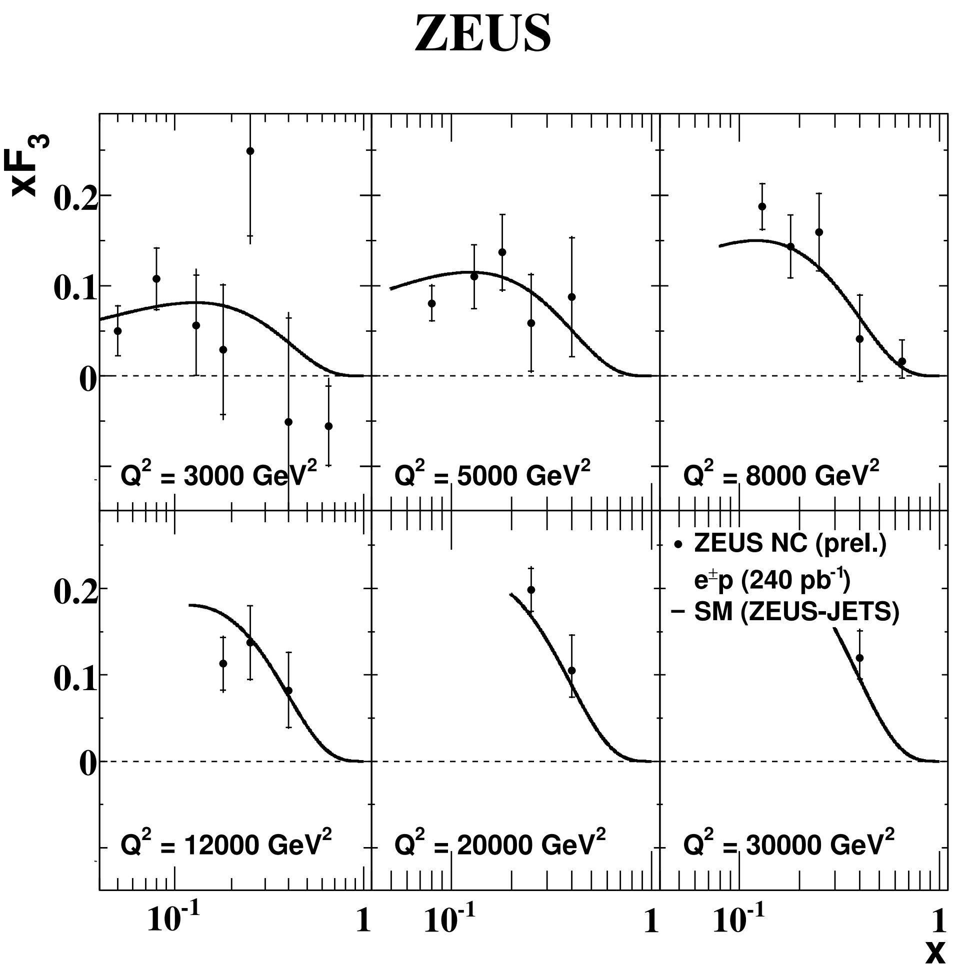

Figure 8: *The structure function xF_3 plotted as a function of x in fixed Q^2 bins. The black dots represent data points and the curves show the predictions of the SM evaluated using the ZEUS-JETS PDFs. The inner error bars show the statistical uncertainty, while the outer ones show the statistical and systematic uncertainties added in quadrature.*

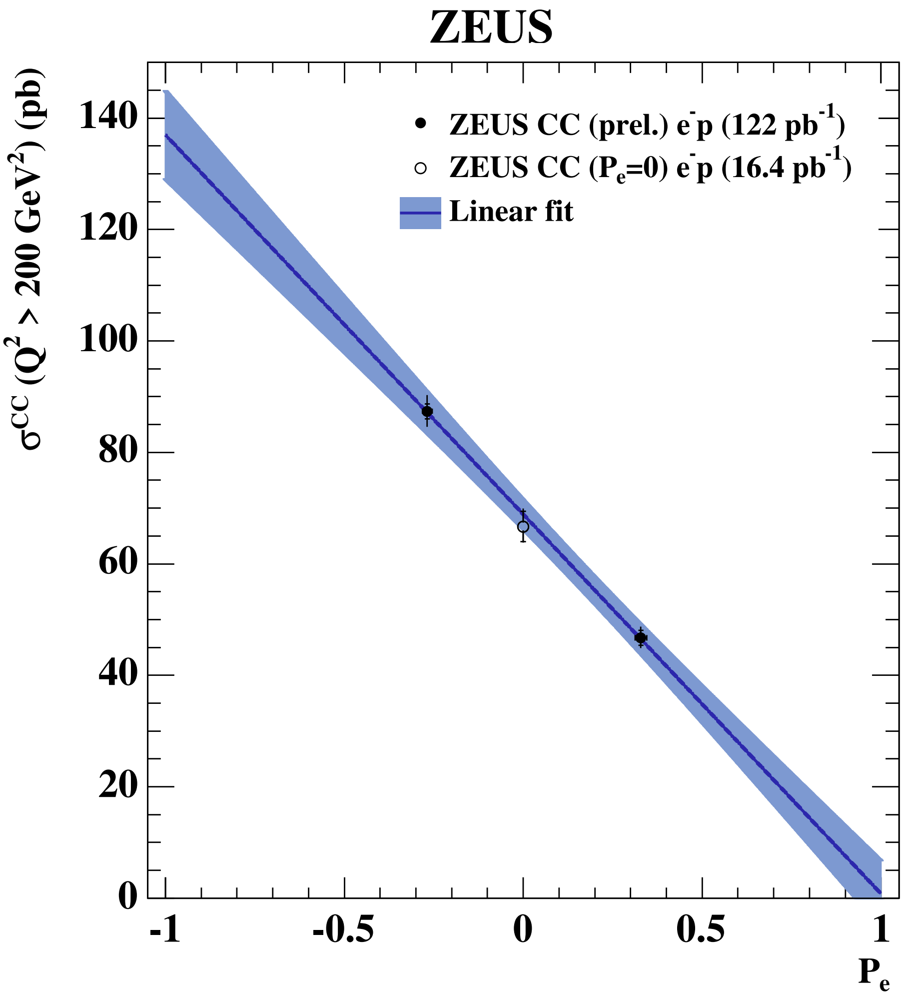

Figure 9: *The total cross section for e^-p CC DIS as a function of the longitudinal polarisation of the electron beam. The line shows the result of a linear fit performed to the three measured points and the shaded area shows the combined statistical and systematic uncertainty on the fit.*

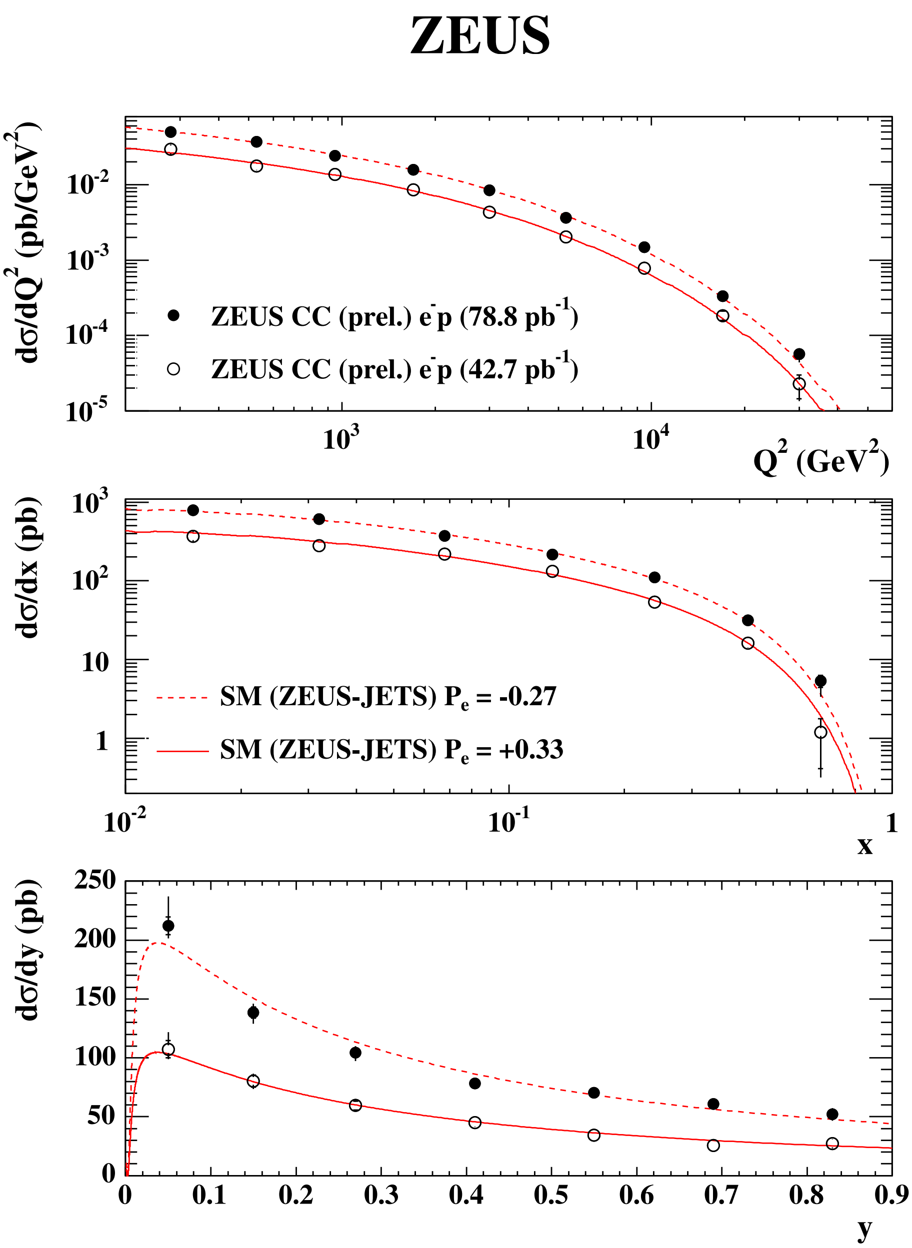

Figure 10: *The $e^{-}p$ CC single differential cross sections $d\sigma/dQ^2$ (top), $d\sigma/dx$ (middle) and $d\sigma/dy$ (bottom). The closed (open) circles represent data points for the negative (positive) polarisation measurements and the curves show the predictions of the SM evaluated using the ZEUS-JETS PDFs.*

ZEUS

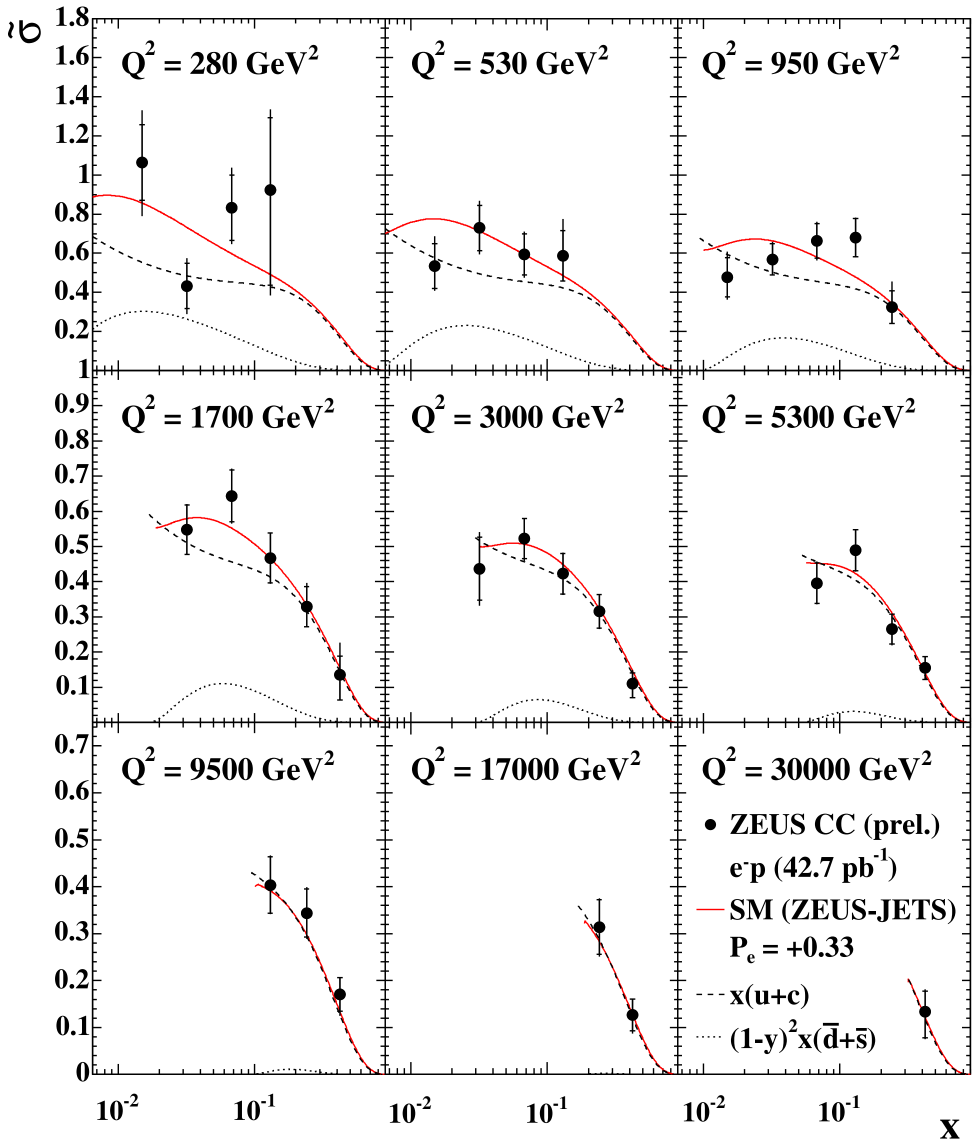

Figure 11: *The e^-p CC DIS reduced cross section plotted as a function of x in bins of fixed Q^2. The circles represent the data points for the positive polarisation measurements and the curves show the predictions of the SM evaluated using the ZEUS-JETS PDFs.*

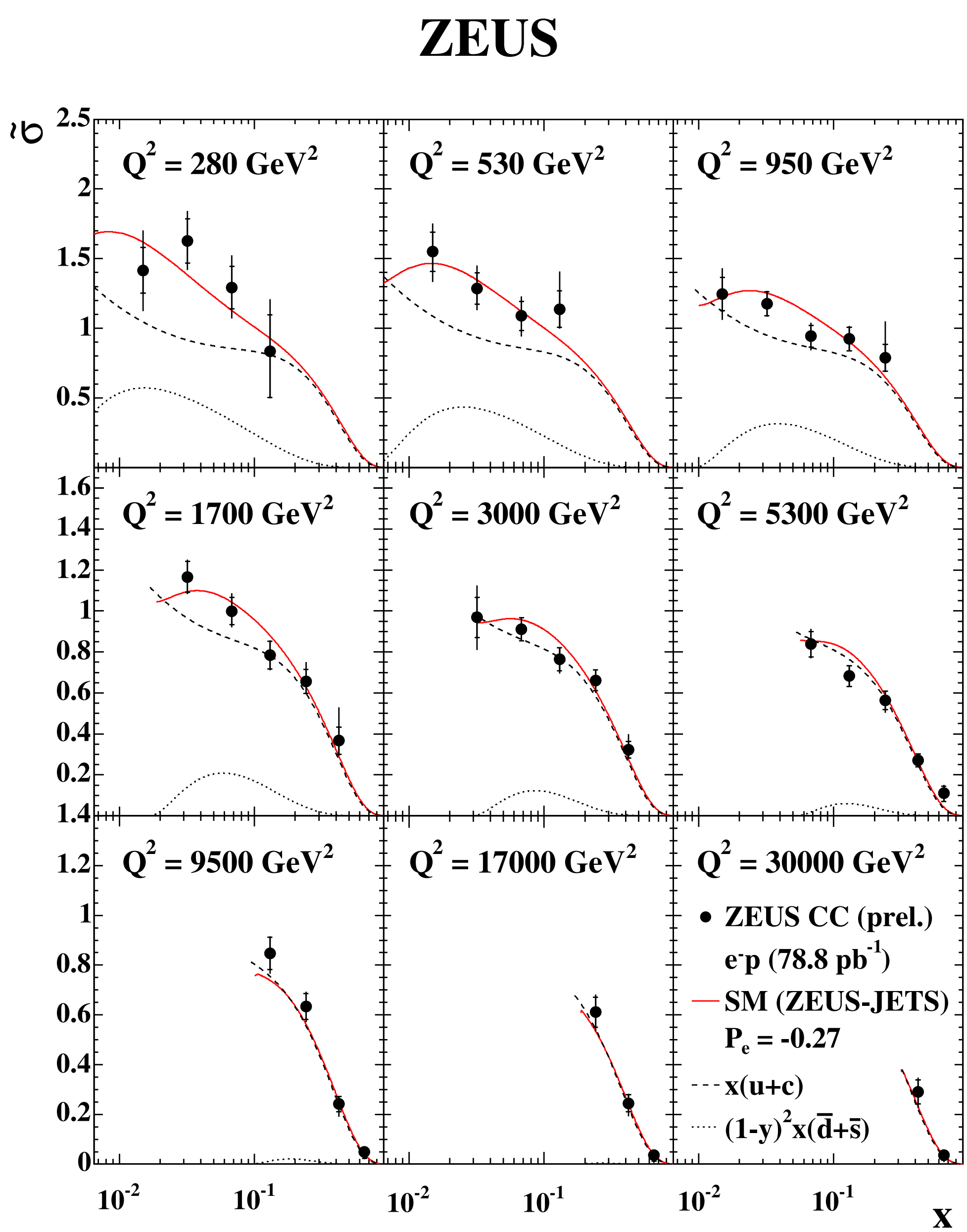

Figure 12: *The e^-p CC DIS reduced cross section plotted as a function of x in bins of fixed Q^2. The circles represent the data points for the negative polarisation measurements and the curves show the predictions of the SM evaluated using the ZEUS-JETS PDFs.*

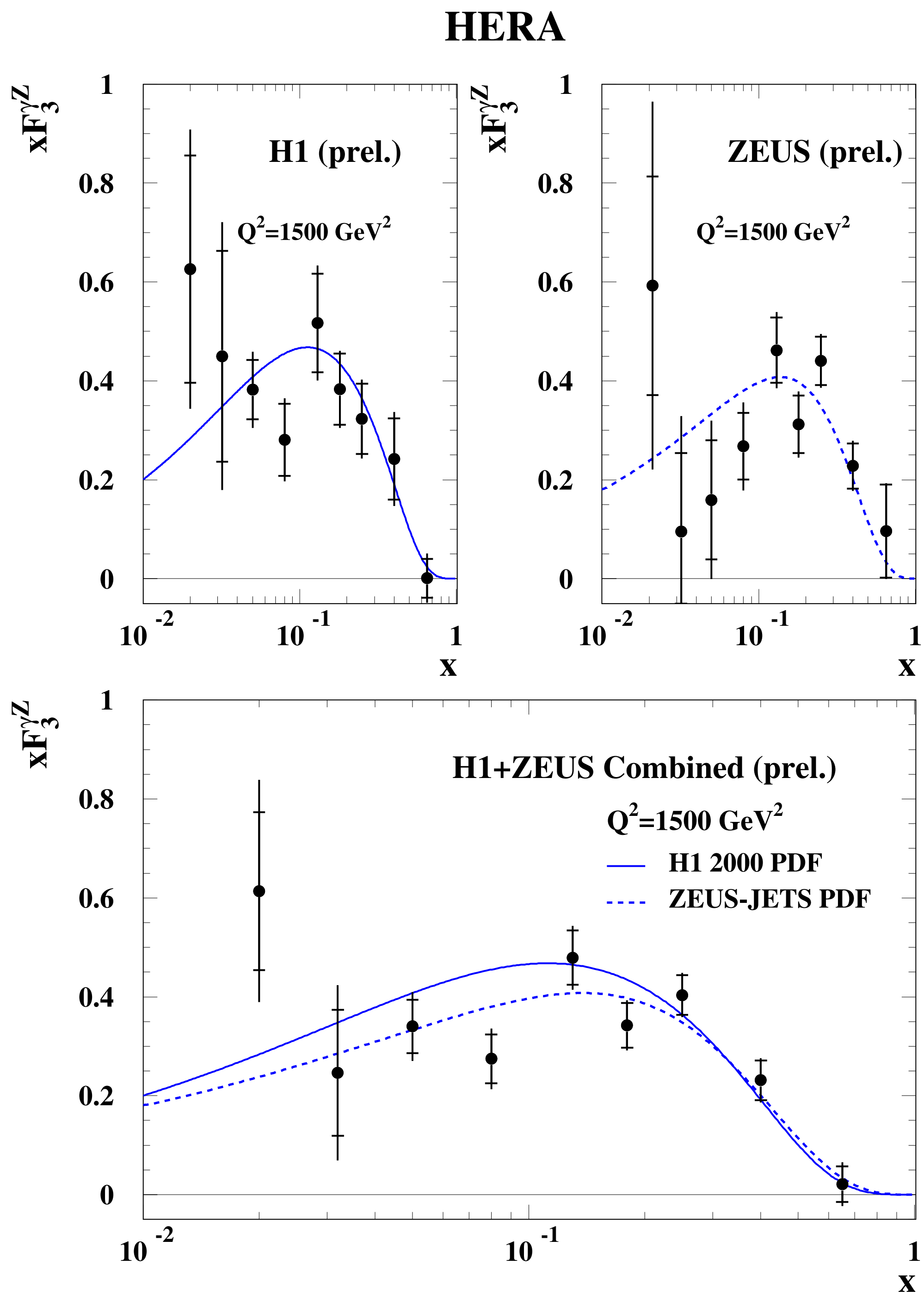

Figure 13: *Measurements of the structure function $xF_3^{\gamma Z}$ by the H1 Collaboration (top left), the ZEUS Collaboration (top right) and combined (bottom). The inner error bars denote the statistical uncertainty while the full error bars comprise the statistical and systematic uncertainty added in quadrature. The curves describe the SM predictions as obtained in NLO QCD fits to H1 inclusive data and to the inclusive and jet ZEUS data, respectively. Both fits have been performed using the unpolarised HERA I data only and they differ in some detail concerning the parameterisations and treatment of the valence quark behaviour.*

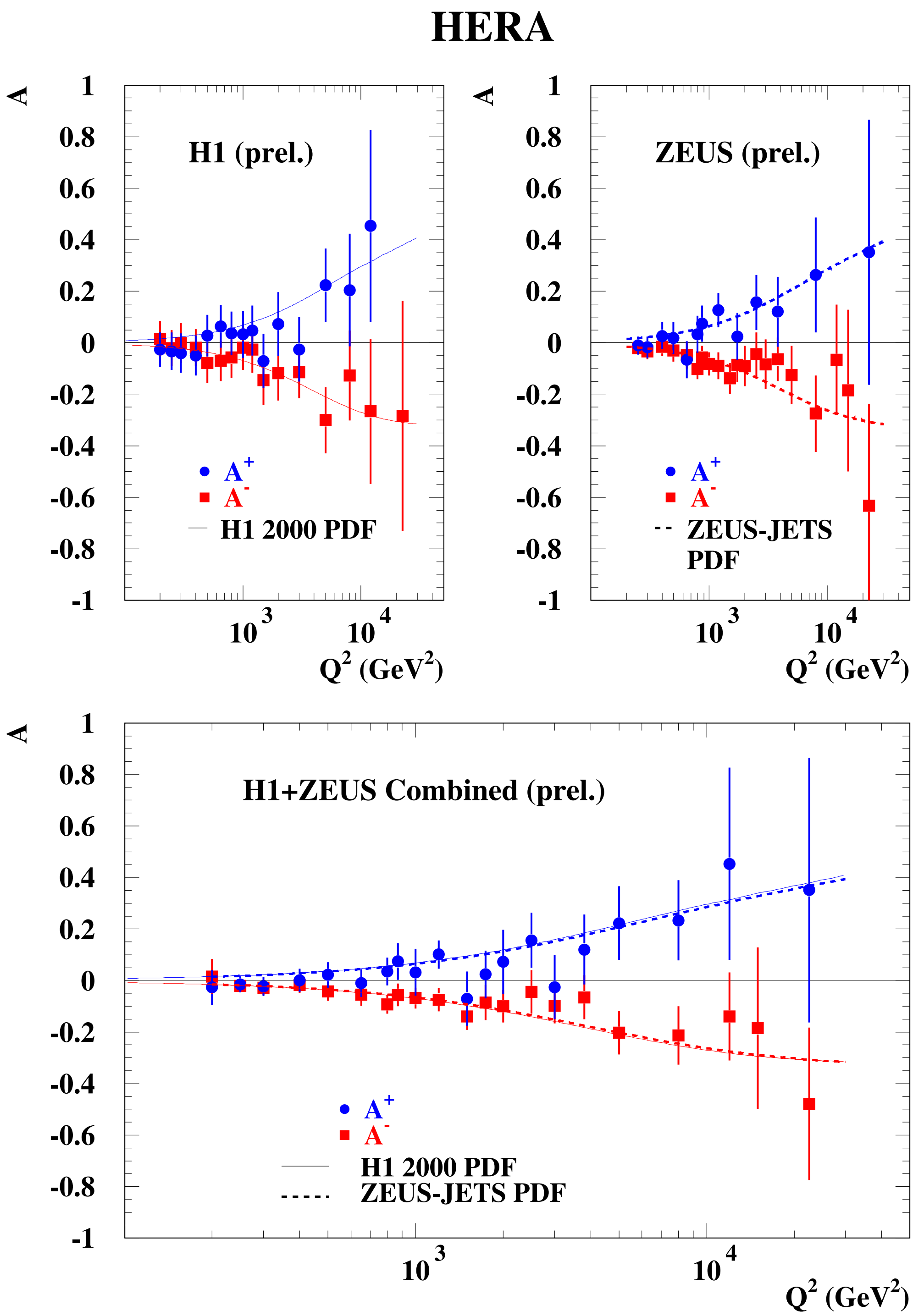

Figure 14: *Measurements of the polarisation asymmetries $A^{\pm}$ by the H1 Collaboration (top left), the ZEUS Collaboration (top right) and combined (bottom). The error bars denote the total uncertainty which is dominated by the uncorrelated error contributions. The curves describe the theoretical predictions in NLO QCD as obtained in fits to the H1 inclusive data and to the inclusive and jet ZEUS data, respectively. Both fits have been performed using the unpolarised HERA I data.*

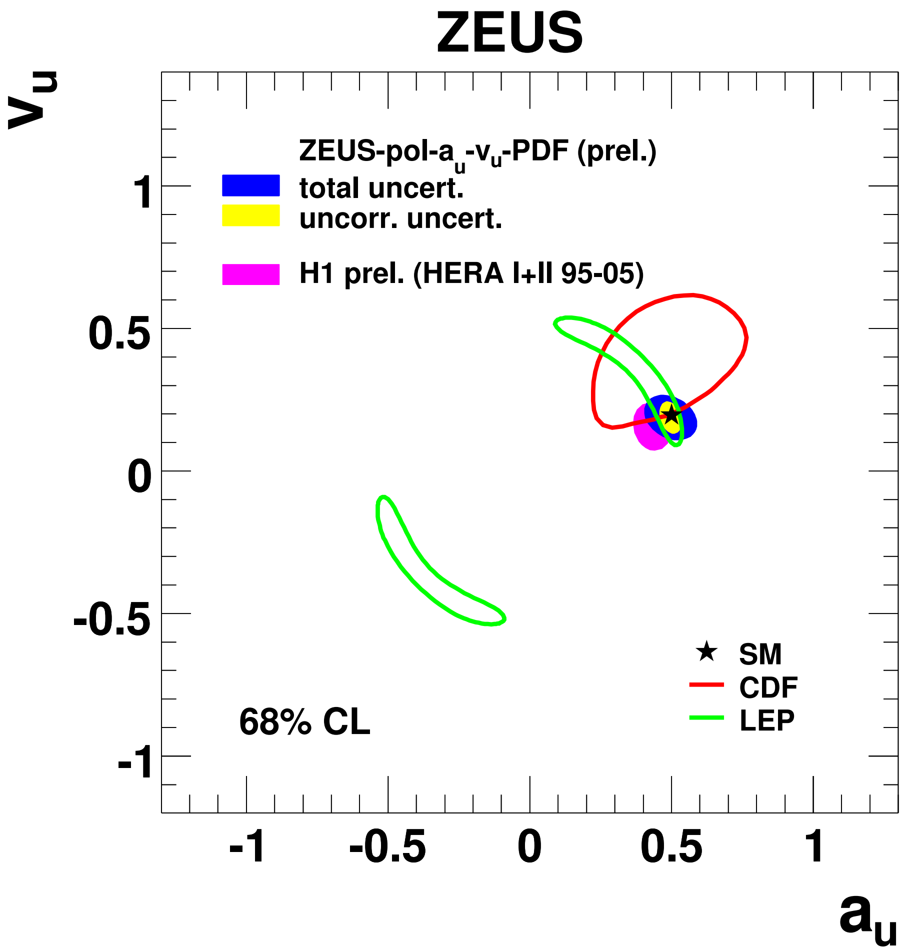

Figure 15: *The 68% confidence level contours for the electroweak parameters a_u and v_u from the ZEUS QCD and EW fit. Also shown are the contours determined by other experiments.*

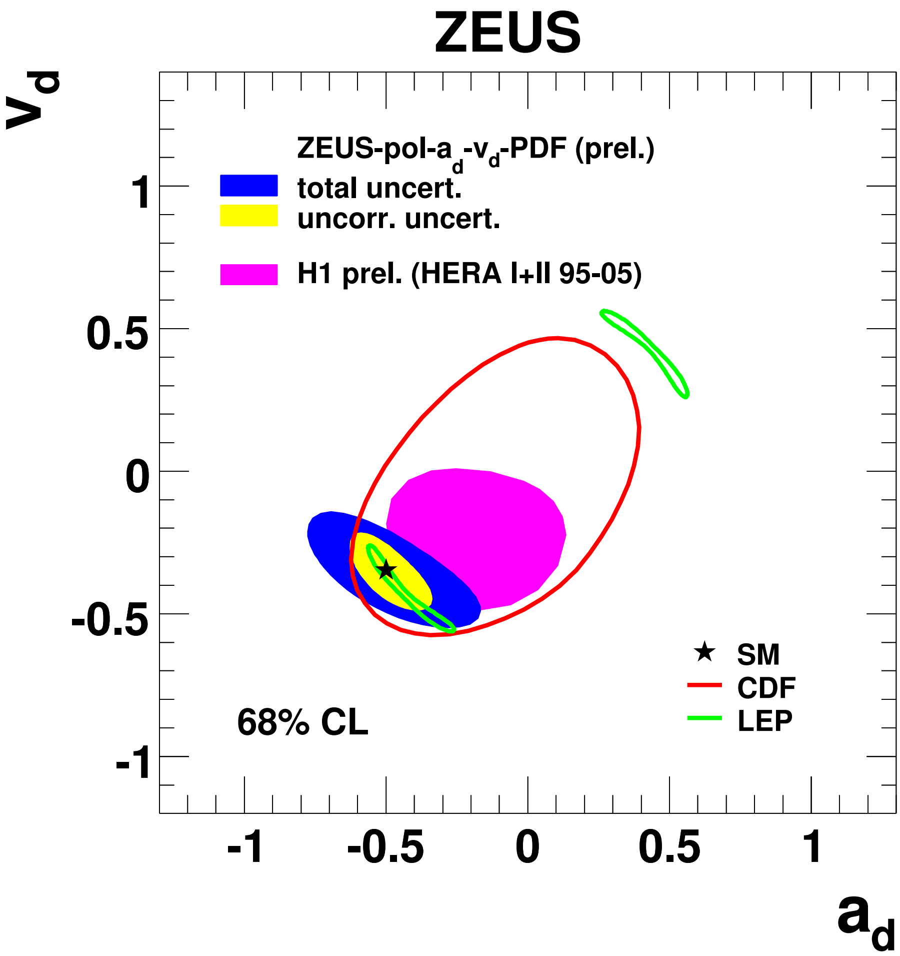

Figure 16: *The 68% confidence level contours for the electroweak parameters a_d and v_d from the ZEUS QCD and EW fit. Also shown are the contours determined by other experiments.*